J Mater Sci (2008) 43:3112–3117
DOI 10.1007/s10853-008-2507-3

The effect of Si and microstructure evolution on the thermal expansion properties of Fe–42Ni–Si alloy strips

M. K. Kim · J. Namkung · Y. S. Ahn

Received: 10 September 2007 / Accepted: 29 January 2008 / Published online: 28 February 2008

Abstract An alloying element of 0–1.5 wt.% Si was added to an Fe–42%Ni system, and alloy strips were fabricated using a melt drag casting process. The effects of the Si and annealing treatments on the thermal expansion properties of Fe–42Ni alloy were investigated. The addition of Si enlarged the coexisting temperature region of the solid–liquid phase and reduced the melting point, which improved the formability of the alloy strip. An alloy containing 0.6 wt.% Si had a lower thermal expansion coefficient than any other alloy in the temperature range from 20 to 350 °C. The grain size increased with the rolling reduction ratio and annealing temperature, which caused an increase in magnetostriction and consequently a decrease in the thermal expansion coefficient of the strip. The alloy strip containing 1.5 wt.% Si had a higher thermal expansion coefficient than the alloy containing 0.6 wt.% Si because of grain refining caused by the precipitation of Ni_3Fe.

Introduction

Fe–Ni alloy has been used in liquefied natural gas (LNG) tanks and materials for electronic parts due to its excellent low-temperature toughness and low thermal expansion coefficient. Applications for this alloy are growing with the development of industrial society and information technology. The alloy is usually fabricated by an ingot-casting process rather than a continuous casting process because continuous casting suitable for mass production can cause hot cracking at the surface and inside Fe–Ni alloy strips [1]. However, ingot casting is uneconomical as it requires a large amount of energy and many different types of equipment. Moreover, it is difficult to control the alloy strip because several factors influence its thermal expansion properties.

It is therefore necessary to develop a new manufacturing process and treatment technique to produce alloy strips having excellent thermal expansion properties. Direct-casting processes such as near-net-shape casting have been introduced to meet current demands [2]. Melt drag casting, which is a type of near-net-shape casting, has been used recently to extend the application of direct-casting methods to various material parts. However, to fabricate Fe–42Ni alloy strips using melt drag casting, a new alloy design is required since the mush zone must be enlarged.

Studies have examined improvements in formability via addition of Mn or S, as well as changes in mechanical and thermal expansion properties with the addition of Co, Mo, V, or B for an optimum Fe–Ni system consisting of 58Fe–42Ni [3]. Since the price of Ni has increased dramatically, studies have sought to reduce the Ni content by substituting low-cost elements. However, a comparable alloy system with excellent thermal expansion properties has not been developed.

In this study, alloy strips composed of Fe–42Ni with 0–1.5% Si content were produced by a melt drag casting process. The effects of the manufacturing conditions and the amount of Si on the thermal expansion properties were investigated.

M. K. Kim · Y. S. Ahn (✉)
School of Materials Science & Engineering, Pukyong National University, Busan 608-739, Korea
e-mail: ysahn@pknu.ac.kr

J. Namkung
New Materials & Component Research Center, Research Institute of Industrial Science & Technology, Pohang 709-330, Korea

Table 1 Chemical composition of the alloys (wt.%)

	Composition
Conventional casting process	57.5Fe–42Ni–0.3Si
	56.9Fe–42Ni–0.6Si
	56Fe–42Ni–1.5Si
Melt drag casting process	57.5Fe–42Ni–0.5Si
	56.9Fe–42Ni–1.0Si
	56Fe–42Ni–1.5Si

Test methodology

Alloy strips were fabricated by commercial ingot and melt drag casting processes. The composition of the alloys is listed in Table 1; each consisted of Fe–42Ni with 1–1.5wt.% Si content. The Fe content was reduced as more Si was added while the Ni content remained constant. To identify an optimum Fe–Ni alloy system for melt drag casting, 30-kg ingots with various Si contents were cast and solution-treated at 1,150 °C for 6 h. The solution-treated strips were hot rolled and cold rolled (reduction rate: 80%) to a thickness of 0.33 mm, followed by recrystallization annealing at 1,150 °C.

To measure the solidus and liquidus temperatures of the alloys, 150-g pins with dimensions of 80 mm × 2Φ were fabricated using a suction equipment. The composition of the pins was Fe–42Ni alloy containing 0–3 wt.% Si. The pins were heated from room temperature to 1,490 °C (heating rate: 10 °C/min) using a DSC (Netzsch Jupiter 449C) analyzer, and the transformation temperatures were measured.

Figure 1 shows a schematic drawing of the melt drag casting process used in this study. Strips were fabricated with a length of 5–10 m, a width of 120 mm, and a thickness of 1.2–1.5 mm. The fabrication conditions during melt drag casting were as follows: casting temperature of 1,490 to 1,520 °C, roll temperature of 25 to 50 °C, roll speed of 0.25–0.5 m/s, and roll gab of 1.2–1.7 mm. The oxidized surface film of the melt drag cast strips was removed by mechanical grinding, and solution annealing at 1,150°C was performed for 3 h under a vacuum atmosphere of 1×10^{-5} torr. The strips were cold rolled to a thickness of 0.33–0.4 mm (reduction ratio: 75–80%), and finally recrystallization annealed in the temperature range of 850–1,150 °C for 30 min.

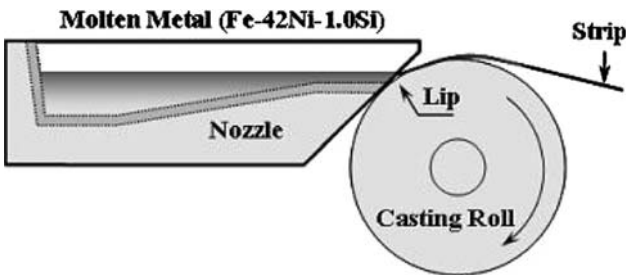

Fig. 1 Schematic drawing of the melt drag casting process

After recrystallization heat treatment at 850, 950, 1,050, or 1,150°C, the thermal expansion properties of the specimens ($l = 10$ mm, $w = 3$ mm) were examined using an R&B dilatometer. We applied a magnetic field of 5 kA/m to a solenoid coil to measure the magnetostriction according to the annealing conditions. The changes in length of the specimen ($\Delta l/l$) resulting from changes in the magnetic flux density induced by the magnetic field were measured using a linear variable differential transformer (LVDT).

Results and discussion

Effect of Si addition on ΔT

The liquid–solid coexisting temperature (ΔT) of an Fe–Ni binary alloy system is less than 5 °C [4]. Such a small ΔT makes it extremely difficult to control the melt flow and the formation of the strip.

Figure 2 shows the variation in the liquidus and solidus temperatures of Fe–Si alloy according to the Si content. The melting point of the alloys decreased from 1,450 to 1,350°C with increasing Si from 0 to 3 wt.% Si, with a sharp ΔT increase from 5 to 58 °C, which should create better process conditions for melt drag casting.

The casting ability of a melt drag process is not determined only by the ΔT. For example, pure Sn has good strip formability during melt drag casting despite a very small ΔT. Pure Sn has low solidification contraction and good volume contraction behavior in the solid state, which can

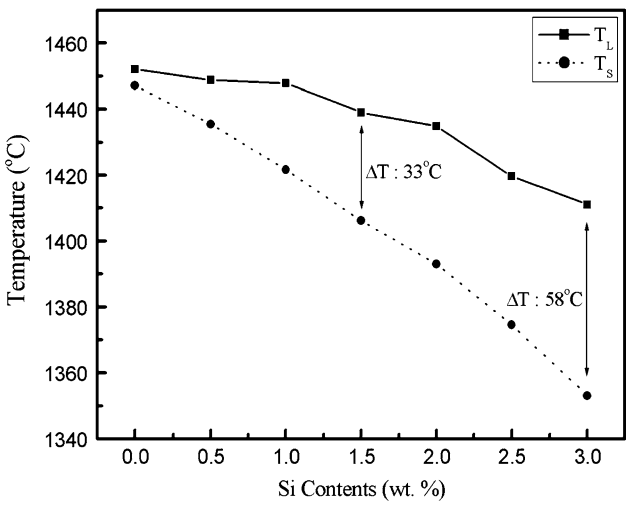

Fig. 2 Liquidus and solidus temperatures as functions of Si content

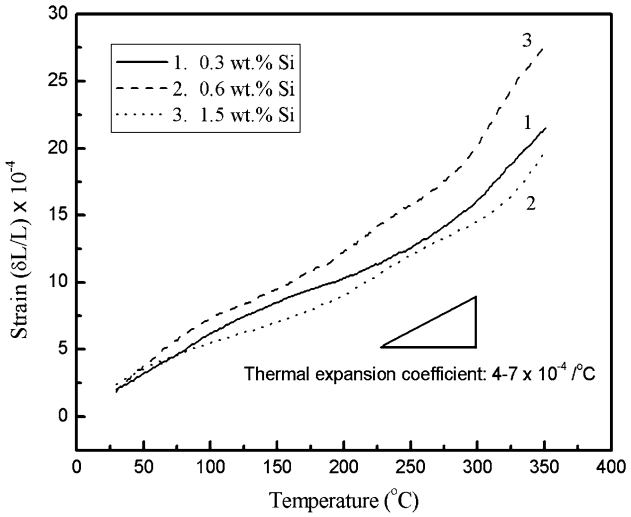

Fig. 3 Thermal expansion of Fe–42Ni alloys with various Si contents fabricated using a conventional process

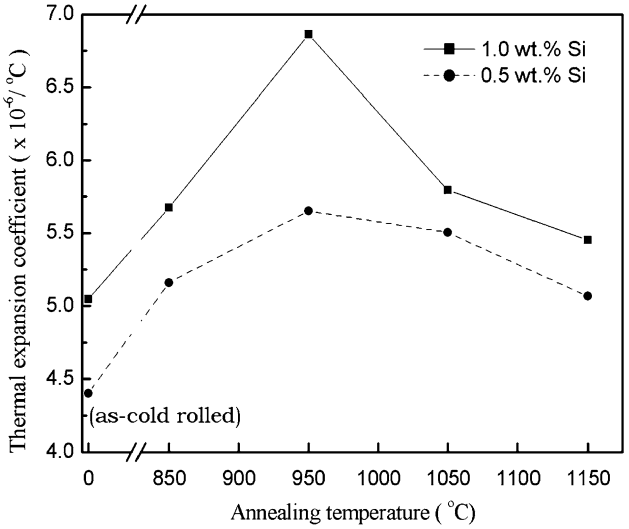

Fig. 4 Thermal expansion coefficients at various annealing temperatures for Fe–42Ni–0.5Si and Fe–42Ni–1Si alloys fabricated using a melt drag casting process

result in good formability during casting. Kocheisen found that the addition of a 0–3.0 wt.% Si alloying element in an Fe–C alloy led to low volume contraction in the solid state [5]. Since Si brought down the melting point and increased the ΔT of an Fe–Ni system, it can also be expected to decrease solidification contraction, which will improve the casting ability and formability of the melt drag process.

Thermal expansion properties of alloy strips

Influence of Si

Figure 3 shows the thermal expansion behavior of the Fe–2Ni alloys fabricated using a commercial casting process, cold rolled, and then recrystallization heat treated at 1,150 °C for 1 h. The thermal expansion behavior was measured during heating from room temperature to 350°C. The commercially cast alloy containing 0.6 wt.% Si had the lowest thermal expansion coefficient (α) of 4×10^{-6}, while the alloy containing 1.5 wt.% Si had the highest value of 7×10^{-6}.

Figure 4 shows the α-values of Fe–42Ni alloy strips containing 0.5% and 1.0% Si. These alloys were melt drag cast, cold rolled, and recrystallization annealed at 850, 950, 1,050, and 1,150 °C, respectively. The as-cold rolled strip had the lowest α compared to the other alloys. The value of α increased with the annealing temperature up to 950 °C and then decreased inversely with temperatures above 950 °C. The reason for this will be discussed in the next section.

Microstructure evolution of the alloys

Figure 5 shows the microstructures of the cast strips after annealing at 950 °C for 30 min. The alloy containing 0.6 wt.% Si had the largest grains, while the 1.5 wt.% Si alloy had the finest grains. Transmission electron microscope (TEM) images of the specimens are shown in Fig. 6. Numerous fine precipitates are visible in the microstructure of Fe–42Ni–1.5Si in Fig. 6c, while no precipitate was found in the alloys containing 0.3 wt.% Si and 0.6 wt.% Si (Fig. 6a, b). These precipitates were identified as Ni_3Fe using X-ray diffraction (XRD), as shown in Fig. 7. The Ni_3Fe phase was formed only when 1.5 wt.% Si was added. Therefore, excessive addition of Si promoted the formation of Ni_3Fe in the alloy, which is known to restrain recrystallization and grain growth. Goman'kov et al. [6] found that substituting Si or Ge for Ni in an Fe–Ni alloy system made the Ni_3Fe lattice stable [6].

The thermal expansion behavior of Fe–Ni Invar alloy can be explained as follows. This alloy expands during heating due to lattice expansion, similar to other alloys. However, in addition, below the Curie temperature (T_c) large negative volume magnetostriction is caused by spontaneous magnetization, which results in a low thermal expansion coefficient for the alloy [7–10]. The magnetostriction increases with the intensity of magnetization and the arrangement of the magnetic domain. The thermal expansion coefficient of Invar alloys, however, increases linearly at temperatures above T_c due to both lattice expansion and thermal perturbation from the arrangement of the magnetic spin.

The Fe–42Ni–0.6Si alloy had a lower thermal expansion coefficient than the Fe–42Ni–0.3Si or Fe–42Ni–1.5Si alloys, as shown in Fig. 3, because it had more negative magnetostriction resulting from the easier movement and rotation of the magnetic domain due to grain coarsening, as

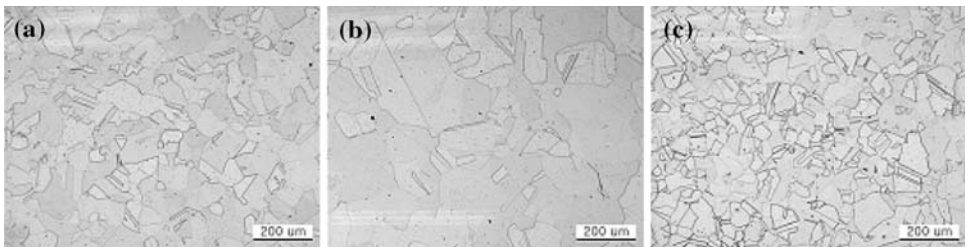

Fig. 5 Microstructures of the Fe–42Ni–*x*Si alloys annealed at 1,150 °C for 30 min and then cold rolled (**a**) Fe–42Ni–0.3Si; (**b**) Fe–42Ni–0.6Si; (**c**) Fe–42Ni–1.5Si

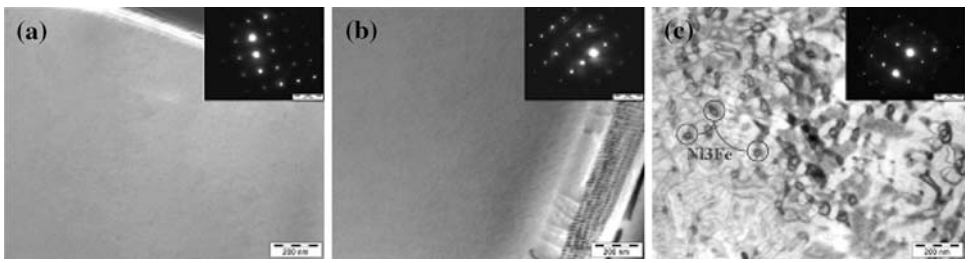

Fig. 6 TEM micrographs of the Fe–42Ni–*x*Si alloys annealed at 1150°C. The precipitates shown in (**c**) were identified as Ni_3Fe using XRD. (**a**) Fe–42Ni–0.3Si; (**b**) Fe–42Ni–0.6Si; (**c**) Fe–42Ni–1.5Si

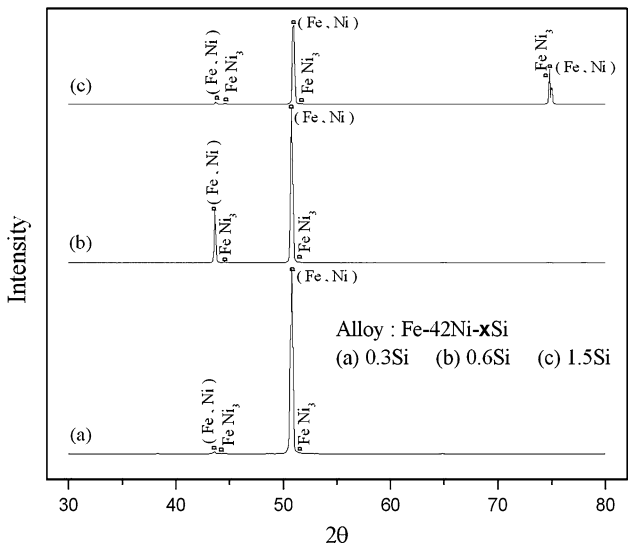

Fig. 7 XRD of Fe–42Ni–*x*Si alloys with various Si contents fabricated using an ingot-casting process

shown in Fig. 5. Grain boundaries act as barriers to the movement and rotation of magnetic domains. The Fe–42Ni–1.5Si alloy had the lowest thermal expansion coefficient because it had the finest grain size. The fine grains in the 1.5 wt.% Si alloy were caused by restraint of grain growth due to the precipitation of Ni_3Fe during the recrystallization heat treatment, as shown in Figs. 6 and 7.

Effect of the annealing conditions

Figure 8 shows the microstructures of an Fe–42Ni–1Si alloy strip annealed for 30 min before the melt drag casting process. In Fig. 8a, the recrystallization is just beginning at 850 °C. The grain size increased with the annealing temperature up to 1,150 °C due to the grain growth.

Figure 9 shows the XRD patterns of the Fe–42Ni–1Si alloy. Here, the (111)-plane peak for Fe or Ni should be the main peak. Deformation due to cold rolling reduced the (111)-plane peak and increased peaks equivalent to the (200) and (220) planes with the rolling reduction rate (Fig. 9a, b). The relative peak intensity of the (111) plane was increased by the recrystallization heat treatment due to the formation of the recrystallization texture during annealing. The peak intensity also increased with the annealing temperature, as shown in Fig. 9c–f.

The as-cold rolled alloy had the lowest thermal expansion coefficient because the texture for magnetization was developed during cold working. Moreover, magnetization of single-crystal Fe is easiest in the [100] direction [11]. Kim and Choi [12] measured the (200) pole figure texture of an Fe-Ni alloy and found that the intensity of a {100}<100> system developed significantly with the rate of cold rolling.

The alloy annealed at 850 °C had a relatively low thermal expansion coefficient because the rolling texture, which developed in the [100] direction, was not dissolved completely at the annealing temperature. Therefore, the alloy could be easily magnetized. The alloy annealed at 950 °C was completely recrystallized and had fine grain structure; therefore, it was hard to magnetize and consequently had a high thermal expansion coefficient. With a further increase in annealing temperature to 1,150 °C, the alloy could be easily magnetized again due to grain growth, which reduced the thermal expansion coefficient. This explains why the alloy annealed at 950 °C had the highest thermal expansion coefficient (see Fig. 4).

Figure 10 shows the magnetostriction ($\lambda(\Delta\ell/\ell)$) properties with increasing magnetic flux density for different annealing temperatures. The figure indicates only positive magnetostriction because alternating current was applied to

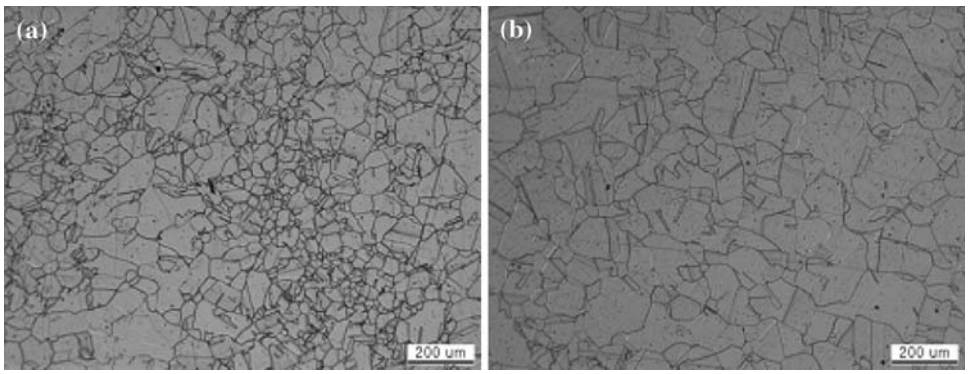

Fig. 8 Microstructures of an Fe–42Ni–1Si alloy strip annealed for 30 min at (**a**) 850 °C and (**b**) 950 °C before the melt drag casting process

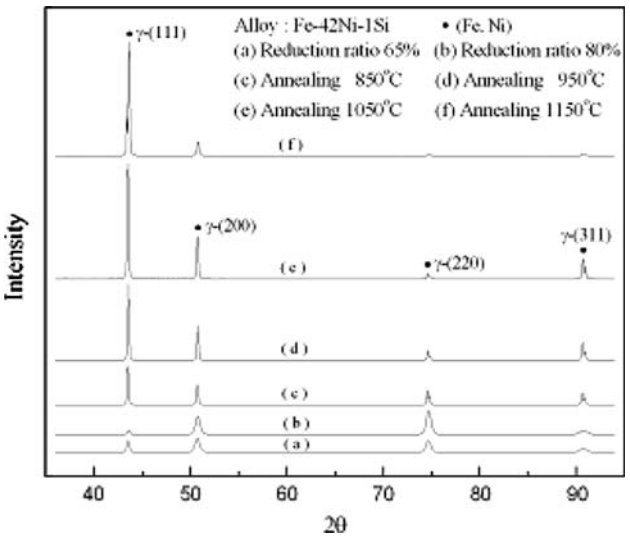

Fig. 9 XRD of the Fe–42Ni–1.0Si alloy strip that was cold rolled (**a** and **b**) and annealed at various temperatures (850–1,150°C: **c**–**f**) before the melt drag casting process

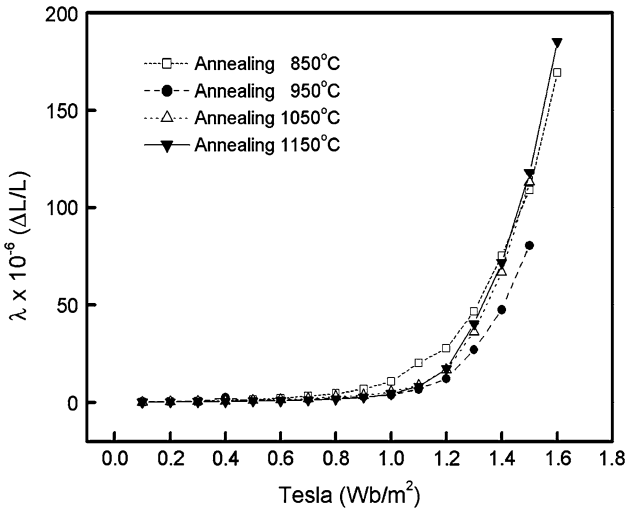

Fig. 10 Magnetostriction of Fe–42Ni–1.0Si alloys annealed at various temperatures

the solenoid coil. The alloy annealed at 950 °C had the lowest magnetostriction since recrystallization was just completed, and the motion and rotation of the magnetic domain were restricted by the high grain boundary density. The alloy annealed at 1,150 °C had the lowest thermal expansion coefficient due to the high magnetostriction caused by the coarse grain.

Conclusions

The following conclusions were drawn from this study.

(1) The addition of a Si alloying element in low expansion Invar alloy of Fe–42Ni increased the coexisting temperature (ΔT) of the liquid–solid phase considerably and decreased the melting point, resulting in good conditions for melt drag casting.

(2) The Fe–42Ni alloy containing 0.6 wt.% Si had the largest grain size and the lowest thermal expansion coefficient. The alloy with 1.5wt.% Si had a smaller grain size and a higher thermal expansion rate than the Fe–42Ni–0.6Si alloy. This was caused by the formation of a Ni_3Fe phase, which restricted recrystallization and grain growth and consequently increased the magnetic anisotropy.

(3) The thermal expansion coefficient of the melt drag cast alloy strip decreased with the rolling reduction rate, increased after the recrystallization annealing treatment, and decreased with increasing annealing temperature. This occurred because the magnetostriction increased with the magnetization of the alloy, improving the thermal expansion properties.

References

1. Kim SK (2002) J Kor Inst Met Mater 40:419
2. International Iron and Steel Institute (1993) Near net shape casting. Brussels
3. Mostefa LB, Saindrenan G, Solignac MP, Colin JP (1991) Acta Mater 39:3111

4. Cacciamani G, De Keyzer J, Ferro R, Klotz UE, Lacaze J, Wollants P (2006) Intermetallics 14:1312
5. Kocheisen K (1972) Giessereiforschung 24:133
6. Goman'kov VI, Puzei IM, Loshmanov AA, Mal'tzev YI (1969) Phys Met Metallogr 28:77
7. Gehrmann B, Acet M, Herper HC, Wassermann EF, Pepperhoff W (1999) Phys Stat Sol (b) 214:175
8. Kim CD, Matsui M, Chikazumi S (1978) J Phys Soc Japan 44:1152
9. Khmelevskyi S, Mohn P (2004) Phys Rev B 69:14
10. Lambret E, Saindrenan G (1996) In: Wittenauer J (ed) Proc. Int. Symposium on the Invar Effect, Paolo Alto, California, pp 39–62
11. Bozorth BM (1986) Ferromagnetism. D. Van Nostrand, New York, p 138
12. Kim YH, Choi SJ (1990) J Kor Inst Met Mater 28:6